Exploring lithium bonding interactions between noble-gas hydrides HXeY and LiX molecules (Y = H, CN, NC and X = H, CN, NC, OH, NH 2 , CH 3): A theoretical study

DATASET *in* COMPUTATIONAL AND THEORETICAL CHEMISTRY · OCTOBER 2013

Impact Factor: 1.55 · DOI: 10.1016/j.comptc.2013.10.026

3 AUTHORS, INCLUDING:

Mehdi D Esrafili
University of Maragheh
180 PUBLICATIONS **901** CITATIONS
SEE PROFILE

Mohammad Solimannejad
Arak University
167 PUBLICATIONS **1,589** CITATIONS
SEE PROFILE

Computational and Theoretical Chemistry 1027 (2014) 84–90

Contents lists available at ScienceDirect

Computational and Theoretical Chemistry

journal homepage: www.elsevier.com/locate/comptc

Exploring lithium bonding interactions between noble-gas hydrides HXeY and LiX molecules (Y = H, CN, NC and X = H, CN, NC, OH, NH_2, CH_3): A theoretical study

Mehdi D. Esrafili [a,*], Parisa Juyban [a], Mohammad Solimannejad [b]

[a] Laboratory of Theoretical Chemistry, Department of Chemistry, University of Maragheh, Maragheh, Iran
[b] Quantum Chemistry Group, Department of Chemistry, Faculty of Sciences, Arak University, Arak 38156-8-8349, Iran

ARTICLE INFO

Article history:
Received 8 September 2013
Received in revised form 31 October 2013
Accepted 31 October 2013
Available online 8 November 2013

Keywords:
Lithium bond
Noble-gas hydride
Ab initio
QTAIM
Electrostatic

ABSTRACT

Quantum chemical calculations were performed to analyze the existence of intermolecular lithium bond interactions in HXeY (Y = H, CN, NC) complexes with LiX, where X = H, CN, NC, OH, NH_2, and CH_3. The geometry optimizations between HXeY and LiX were performed with the MP2 and M06–2X methods using aug-cc-pVTZ basis set. One can see that, the H–Xe stretching mode of HXeY molecules shifts upon complexation higher in energy, i.e. exhibits a blue shift. The blue shifts of the H—Xe stretching mode are attributed to the enhancement of the $(HXe)^+Y^-$ ion-pair character upon complexation. The global minimum for the HXeY···LiX complexes was found on the potential energy surface for the structure I, i.e. the structure of a linear Xe–Y···Li interaction. It is seen that the lithium bond interaction energies span over a range from −9.5 to −31 kcal/mol at the CCSD(T)/aug-cc-pVTZ level of theory. For the all HXeY···LiX complexes studied, the dominant attractive contributions mostly originate from the electrostatic energy E_{elst}. According to quantum theory of atoms in molecules (QTAIM), all lithium bond interactions studied here display the characters of closed-shell and noncovalent interactions. The redistribution of the electron density at H–Xe critical points upon complex formation is also noticeable, which is in accord with the computed H—Xe frequency shifts in HXeY···LiX complexes.

1. Introduction

Intermolecular interactions play a particular role in chemistry and biochemistry, mainly because they are responsible for stabilizing many important macromolecules, for example, DNA and proteins polymerization reactions [1,2]. The classical hydrogen bond, an example of a strong intermolecular force, has been widely studied over many years and is utilized in crystal engineering as a structural member [3,4]. More recently, other weaker interactions, for example, halogen bonds [5,6], nonclassical hydrogen bonds [7–9] and halogen···halogen interactions [10,11] have been examined with a view to utilization in crystal engineering. Lithium bond (LB) refers to the noncovalent interaction of general structure A-Li···B between lithium-bearing compounds and nucleophiles. Since the first observation in X···Li–Y (X = H_3N, Me_3N, H_2O, Me_2O; Y = Cl, Br) systems by Ault and Pimental in 1975 [12], LB has been widely identified in a variety of systems and the concept of Li-bonding has become important in many fields [13–16].

The discovery of compounds containing noble-gas atoms by experimental and computational techniques has stimulated intensive studies of these molecules and related compounds. Many of these newly discovered molecules are of the form HNgY, where Ng is a noble-gas and Y is an electronegative fragment [17–20]. These compounds, noble-gas hydrides, often contain either xenon or krypton and are made primarily by matrix isolation [21,22]. The first and only ground-state molecule with argon (HArF) was successfully synthesized in 2000 using a low-temperature matrix-isolation technique [23]. Although no stable compounds containing helium or neon have been characterized experimentally, quantum chemical calculations predict that some of them could possibly be synthesized [24,25]. The HNgY molecules are chemically bound systems and their stability are essentially governed by the $(H—Ng)^+Y^-$ ion-pair character, where $(H—Ng)^+$ is covalent, and the interaction between $(HNg)^+$ and Y^- is mainly ionic [19]. Due to such an ionic character, the HNgY compounds are expected to be highly reactive, as verified by the large splitting of their vibrational bands between different solid state configurations [26].

To date, a number of complexes between noble-gas hydrides and other molecules have been experimentally [27–31] and computationally [32–39] studied. The experimental findings ignited computational studies of various HNgY complexes reviewed in

* Corresponding author. Address: Laboratory of Theoretical Chemistry, Department of Chemistry, University of Maragheh, P.O. Box 5513864596, Maragheh, Iran. Tel.: +98 4212237955; fax: +98 4212276060.
E-mail address: esrafili@maragheh.ac.ir (M.D. Esrafili).

2210-271X/$ - see front matter © 2013 Elsevier B.V. All rights reserved.
http://dx.doi.org/10.1016/j.comptc.2013.10.026

detail by McDowell [40] and Lignell et al. [41]. It is revealed that interaction with other molecules and environment has a strong effect on vibrational properties of HNgY molecules due to their weak bonding and large dipole moment. All the experimentally prepared HNgY complexes exhibit blueshifts of the H–Ng stretching mode while theoretical predictions for the FArF···P_2, FArH···HBeH and HArF···HCCH show the H–Ar stretching redshifts [42,43]. Apparently the magnitude of the quadrupole moment of the bonding partner determines whether a redshift or a blueshift is obtained in the HArF complexes. A blueshift of ~300 cm^{-1} was observed for the HKrCl···HCl complex, which is probably the largest blue shift reported for 1:1 complexes [44]. The H–Ng stretching blueshift presumably originates from the enhanced $(HNg)^+Y^-$ charge separation upon complex formation [45]. To date, the complexes of HArF [30], HKrF [30], HKrCl [30,44,46], HXeI [29], HXeBr [28,31,47], HXeCl [28,31], HXeCCH [48], and HXeOH [49] have been observed experimentally and the number of calculated complexes is much bigger. Stable complexes of HArF, HKrF, and HKrCl with N_2 were studied by Lignell et al. [27]. Two structures of the complexes seem to be stable, namely a linear and a bent one. An interesting effect is a very large blue shift (>100 cm^{-1} for HKrCl) of the H–Ng stretching frequency in the linear isomer. As a result, there is a stronger H−Kr covalent bond in N_2−HKrCl than in free HKrCl. Quantum chemical calculations suggest that electrostatic interactions dominate in the linear complex, whereas in the bent complex, the electrostatic and dispersion attractions are roughly equal [50].

In the present work, we use a spectrum of quantum chemical methods -DFT, MP2, and CCSD(T)- to analyze the existence of intermolecular LB interactions in HXeY (Y = H, CN, NC) complexes with LiX, where X = H, CN, NC, OH, NH_2, and CH_3. Molecular geometries, interaction energies, topological parameters, and shifts in vibrational frequencies are reported to characterize the nature and properties of the resultant LB interactions. To further understand the origin of the LB interactions, an energy decomposition analysis was also performed. To the best of our knowledge, LB interactions involving HXeH, HXeCN and HXeNC noble-gas hydrides have been reported here for the first time.

2. Computational details

All quantum chemical calculations were carried out using the GAMESS suite of programs [51]. The geometries of all studied complexes were fully optimized with the M06–2X and MP2 methods. A mixed basis set approach was used; here the Xe atom is described using the pseudopotential based aug-cc-pVTZ-PP basis [52] and the aug-cc-pVTZ is used for other atoms. Harmonic frequencies were calculated to confirm the equilibrium geometries that correspond to energy minima. The interaction energies of the all optimized HXeY···LiX complexes were calculated using the MP2, CCSD(T) and M06–2X/aug-cc-pVTZ(-PP) methods, where MP2 optimized geometries were used in the CCSD(T) calculations. They have been computed as the differences between the total energies of the complexes and the energies of the isolated monomers and have been corrected for basis set superposition error (BSSE) using the counterpoise method [53]. The quantum theory of atoms in molecules (QTAIM) [54] analysis was preformed with the help of AIM 2000 software [55] using the wave functions generated at the MP2/aug-cc-pVTZ(-PP) level. The nature of the LB interactions has been explored using the following energy decomposition scheme [56]:

$$E_{int} = E_{elst} + E_{exch-rep} + E_{pol} + E_{disp} \quad (1)$$

where E_{elst}, $E_{exch\text{-}rep}$, E_{pol} and E_{disp} correspond to electrostatic, exchange-repulsion, polarization and dispersion terms, respectively. All the energy decomposition analyses were carried out using GAMESS package [51].

3. Results and discussion

3.1. Geometries and vibrational frequencies

Fig. 1 indicates a sketch of the HXeY···LiX complexes, where Y = H, CN, NC and X = H, CN, NC, NH_2, OH, CH_3. The structure of the HXeY···LiX complexes was optimized at the two levels of theory [MP2/aug-cc-pVTZ(-PP) and M06–2X/aug-cc-pVTZ(-PP)]. All the considered species are found to possess well-defined energy minima. It is known from previous studies [19] that, at their equilibrium geometries, the noble-gas hydrides HNgY feature a covalent H–Ng bond and an ionic interaction, best described by the resonance form $(H–Ng)^+Y^-$. The calculated H–Xe and Xe–Y bond lengths of the isolated HXeH, HXeCN and HXeNC molecules optimized at different computational levels are presented in Table 1. It is notable that the calculations give a shorter H–Xe bond length and also stronger charge separation between H–Xe and Y fragments for HXeNC than for HXeCN. This observation is consistent with the previous work on the HXeCN and HXeNC molecules [18], where a shorter H–Xe distance for NC-isomer was theoretically predicted and experimentally verified by its higher vibrational frequency. From Table 1, it is evident that the molecular properties of HXeY are dependent on the computational level used to describe the molecule. The H–Ng bond distances of HXeY are predicted as 1.855 Å (for Y = H), 2.398 Å (for Y = CN) and 2.330 Å (for Y = NC) at the MP2/aug-cc-pVTZ(-PP) level of theory. However, the H–Xe bond distances calculated using MP2 are consistently shorter than those obtained with M06–2X method by approximately 0.01–0.02 Å. The trend in the equilibrium bond distance between the noble-gas atom and the Y moiety in HXeY is $r_{Xe-H} > r_{Xe-NC} > r_{Xe-CN}$. These facts can be easily understood taking into account the increasing Mullikan charge separation between $(HXe)^+$ and Y^- moieties (+0.3e/−0.3e,+0.6e/−0.6e and +0.7e/−0.7e for the HXeH, HXeNC and HXeCN molecules, respectively).

The computed intermolecular distances of the HXeY···LiX at the M06–2X and MP2/aug-cc-pVTZ(-PP) levels are collected in Table 1. Only one stable structure was found for the HXeH···LiX complexes, which corresponds to a linear Xe–Y···Li structure (Fig. 1). On the other hand, the structural optimization of the HXeY···LiX complexes (Y = CN, NC and X = H, CN, NC) at the both levels of theory yields two minima on the potential energy surface. Structure I is stabilized by the linear Y···Li interaction. Structure II comprises the interaction between the electron-rich environment of a π bond and Li atom (Li···π interaction). From Table 1, it is apparent that the estimated LB distances of structures I are in a range of 1.854–1.922, 1.977–2.019 and 2.109–2.150 Å for HXeH···LiX, HXeCN···LiX and HXeNC···LiX complexes, respectively. These are much smaller than the sum of Van der Waals radii for counterpart atoms [57], which reveals the existence of the relatively strong interaction between HXeY and LiX molecules. The evaluated Li···π bond distances of configuration II are in the range of 2.339–2.535 Å (MP2) and 2.291–2.490 Å (M06). The binding distance in the linear

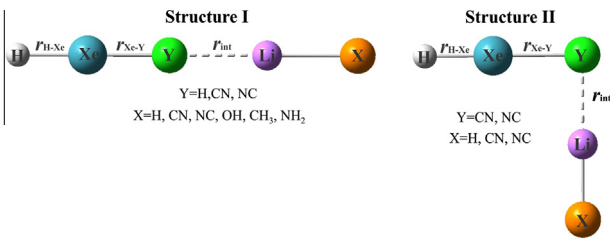

Fig. 1. Structure of HXeY···LiX complexes.

Table 1
Calculated bond lengths (in Å), $\nu_{H\text{-}Xe}$ harmonic frequencies (in cm^{-1}) and corresponding intensities (in km/mol) for HXeY and HXeY···LiX complexes.

Complex	MP2					M06–2X				
	r_{int}	$r_{Xe\text{-}Y}$	$r_{H\text{-}Xe}$	$\nu_{H\text{-}Xe}$	$I_{H\text{-}Xe}$	r_{int}	$r_{Xe\text{-}Y}$	$r_{H\text{-}Xe}$	$\nu_{H\text{-}Xe}$	$I_{H\text{-}Xe}$
HXeH	–	1.855	1.855	1302	2249	–	1.865	1.865	1331	2602
HXeH···LiH (I)	1.913	1.933	1.752	1319	3841	1.889	1.963	1.761	1314	3836
HXeH···LiCN (I)	1.855	1.955	1.734	1335	3516	1.837	1.985	1.743	1396	3253
HXeH···LiNC (I)	1.854	1.957	1.734	1335	3510	1.842	1.983	1.745	1396	3290
HXeH···LiOH (I)	1.922	1.925	1.760	1331	3241	1.910	1.953	1.769	1300	3175
HXeH···$LiNH_2$ (I)	1.914	1.927	1.758	1332	3354	1.902	1.952	1.768	1342	3193
HXeH···$LiCH_3$ (I)	1.911	1.930	1.755	1330	3597	1.900	1.958	1.764	1304	3512
HXeCN	–	2.398	1.691	1863	1030	–	2.426	1.701	1990	757
HXeCN···LiH (I)	2.003	2.475	1.656	1943	547	1.968	2.506	1.672	2003	423
HXeCN···LiH (II)	2.402	2.433	1.679	1916	537	2.387	2.450	1.692	1881	400
HXeCN···LiCN (I)	1.979	2.493	1.651	1969	474	1.945	2.525	1.667	1991	359
HXeCN···LiCN (II)	2.339	2.440	1.671	1956	447	2.291	2.468	1.680	2026	326
HXeCN···LiNC (I)	1.977	2.493	1.651	1966	482	1.950	2.524	1.667	1992	370
HXeCN···LiNC (II)	2.342	2.442	1.670	2000	439	2.297	2.462	1.679	2030	329
HXeCN···LiOH (I)	2.019	2.467	1.659	1929	590	1.994	2.497	1.675	2009	448
HXeCN···$LiNH_2$ (I)	2.016	2.469	1.659	1931	596	1.989	2.499	1.674	2008	453
HXeCN···$LiCH_3$ (I)	2.010	2.472	1.657	1942	588	1.978	2.503	1.672	1983	451
HXeNC	–	2.330	1.646	2102	241	–	2.344	1.664	1992	544
HXeNC···LiH (I)	2.137	2.398	1.625	2116	198	2.117	2.415	1.641	2087	195
HXeNC···LiH (II)	2.535	2.434	1.639	2121	153	2.490	2.373	1.660	2085	218
HXeNC···LiCN (I)	2.109	2.414	1.622	2135	156	2.092	2.433	1.637	2125	153
HXeNC···LiCN (II)	2.492	2.355	1.632	2168	147	2.408	2.448	1.654	2029	136
HXeNC···LiNC (I)	2.109	2.415	1.622	2136	168	2.096	2.430	1.637	2042	148
HXeNC···LiNC (II)	2.494	2.353	1.633	2163	143	2.410	2.447	1.655	2025	136
HXeNC···LiOH (I)	2.150	2.391	1.627	2106	225	2.134	2.406	1.643	2079	217
HXeNC···$LiNH_2$ (I)	2.146	2.393	1.627	2105	224	2.131	2.408	1.643	2223	423
HXeNC···$LiCH_3$ (I)	2.144	2.395	1.626	2112	219	2.121	2.411	1.641	2098	217

HXeH···LiH complex is calculated to be 1.913 Å and 1.889 Å at the MP2 and M06/aug-cc-pVTZ levels of theory, respectively. This value corresponds nicely with other Li-hydride bond studies which reported an average distance of 1.8 Å [15]. It is seen from Table 1 that the presence of the electron-donating groups makes an increase of binding distance. More especially, the substitution of electron-donating groups (OH and NH_2) in the HXeCN···LiX makes a 0.016 and 0.013 Å increase of the binding distance, respectively, whereas the electron-withdrawing groups (CN and NC) result in a 0.024 and 0.026 Å decrease of the binding distance. Upon complexation of HXeY, the build-up of negative charges on the Y involved in the interaction also increases the ionic as well as covalent nature of the particular Xe–Y and H–Xe bonds, respectively. It is evident that the formation of the complexes results in lengthening of the Xe–Y and shortening of the H–Xe bond for the all structures. For the HXeY···LiX complexes (Y = CN, NC and X = H, CN, NC), the lengthening of the Xe–Y bond in structure I is larger than that in structure II. Similar results are also obtained for the H–Xe bond length. The shortening is larger for the strongest structure I than for structure II. For example, the shortening of the H–Xe bond in structure I of HXeY···LiH (0.035 at MP2) is larger than that in structure II (0.001 Å at MP2).

The calculated vibrational frequencies and their intensities for the H–Xe stretching mode are presented in Table 1. As can be expected based on the computed H–Xe bond distances, the vibrational frequencies are varying heavily based on the computational level. In addition, consistent with the covalent character of the H–Xe bonds, the corresponding stretching frequencies are particularly high. The MP2 harmonic H–Xe stretching frequencies are 1302, 1863 and 2102 cm^{-1} for the strongest (asymmetric) stretching band of HXeH, HXeCN and HXeNC, respectively. These frequencies are higher than the experimental values of 1166, 1624 and 1881 cm^{-1} [18,22], respectively. However, relatively high H–Ng stretching frequencies obtained with the harmonic approximation are common for noble-gas hydrides [31]. One can see that, the H–Xe stretching mode of HXeY molecules shifts upon complexation higher in energy, i.e. exhibits a blue shift. For structure I, the complexation-induced blue shifts of H–Xe stretching mode are the largest at the MP2 and M06 levels. The blueshifts of the H–Xe stretching mode are attributed to the enhancement of the $(HXe)^{+}$ Y^{-} ion-pair character upon complexation [45]. This charge redistribution should correlate with the shortening of the H–Xe bond and the blueshifts of its vibrational frequency (Fig. 2). As a result, there is a stronger H–Xe covalent bond in HXeY···LiX than in free HXeY molecules. Also the large increase of the H–Xe intensity of the HXeH···LiX compared with the isolated HXeH must be noted. For a given X, the enhancement of the H–Xe stretch absorption band of HXeY···LiX is also larger for structure I than II.

It should be noted that in addition to strengthening of H–Ng bonding upon complexation, usually the bending barrier of HNgY molecule becomes weaker due to the increased ionic character of the $(HNg)^{+}Y^{-}$ molecule. The calculated HNgY bending frequencies are collected in Table S1 (Supporting Information). One can see that the complexation typically decreases the HNgY bending frequency and the MP2 calculations predict redshift of 2–27 cm^{-1} compared with the monomer bending vibration. This finding

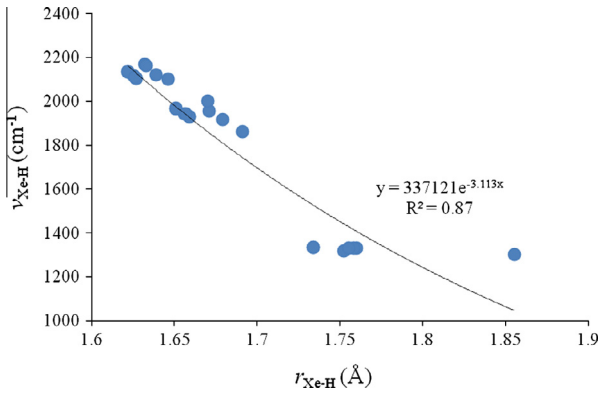

Fig. 2. Relationship between H–Xe bond lengths and IR stretching frequencies.

reveals that Li-bonding interaction between HXeY and LiX molecules tend to weaken the energy barrier of the HNgY → HY + Ng decomposition channel and hence decrease the kinetic stability of HXeY complexes.

3.2. Electron density analysis

A great deal of information about the nature of interactions in the HXeY···LiX complexes can be obtained from topological analysis of its electron density. Based on the QTAIM [54], properties of bond critical points (BCPs) serve to summarize the nature of the interaction between two atoms as shared (covalent) or closed-shell (ionic) interaction. Moreover, the electron density at the BCP, ρ_{BCP}, can well reflect the strength of a bond. Generally speaking, the larger the value of ρ_{BCP}, the stronger the bond will be [54].

The electron density ρ_{BCP} at the LB critical points, the Laplacian of the electron density $\nabla^2\rho_{BCP}$, and the total electron energy density H_{BCP} for the title complexes are presented in Table 2. It is seen that for the Li···H type complexes, the values of ρ_{BCP} are about 0.012. For the Li···N and Li···C types LB complexes, the value of ρ_{BCP} are in the range of 0.026–0.030 and 0.024–0.028 au, respectively. The calculated values of ρ_{BCP} at the Li···π vary from 0.007 to 0.012 au. For all the LB contacts, the small ρ_{BCP} and positive $\nabla^2\rho_{BCP}$ values are essentially consistent with the topological properties of conventional LB interaction [15,16]. It has been manifested in numerous studies [58–60] that the character of interaction could be classified as function of the H_{BCP} with Laplacian of the electron density at BCP ($\nabla^2\rho_{BCP}$). It means that for strong interactions ($\nabla^2\rho_{BCP} < 0$ and $H_{BCP} < 0$) the covalent character is established, for medium strength ($\nabla^2\rho_{BCP} > 0$ and $H_{BCP} < 0$) their partially covalent character is defined, and weak ones ($\nabla^2\rho_{BCP} > 0$ and $H_{BCP} > 0$) are mainly electrostatic. An alternative tool for assessing the nature of interaction is the absolute ratio of kinetic energy and potential energy densities, $-G_{BCP}/V_{BCP}$. Accordingly, if $-G_{BCP}/V_{BCP} > 1$, then the interaction is noncovalent in nature. On the other hand, if $0.5 < -G_{BCP}/V_{BCP} < 1$ then the interaction is partly covalent. For all the studied LBs, $\nabla^2\rho_{BCP}$ and the H_{BCP} values are positive and $-G_{BCP}/V_{BCP}$ values are greater than 1. Thus, all LBs interactions studied here display the characters of "closed-shell" and noncovalent interactions. These results are consistent with the previous interaction energy analysis of HNgY complexes, in which the electrostatic interactions are very important contribution to the total interaction energy [41].

As seen from Table 2, at the BCP of any H–Xe bond, the charge density is rather high, the corresponding Laplacian is negative, and the energy density has a negative value. All these features point to shared-type or covalent interactions. On the other hand, the small values of ρ_{BCP}, the positive values of the $\nabla^2\rho_{BCP}$ and the nearly zero values of H_{BCP} suggest that the all Xe–Y (Y = CN, NC) interactions are weak and basically electrostatic in nature. The redistribution of the electron density at H–Xe critical points upon complex formation is also noticeable. The electron densities at the H–Xe BCPs in the HXeY···LiX complexes are in the range 0.146–0.169 au, which are far larger than those of free HXeY molecules. These findings are also in agreement with the observed blueshift of the stretching and the shortening of the H–Xe bond upon complexation. As a result, there is a stronger H–Xe covalent bond in HXeY···LiX than in free HXeY. On the other hand, it is seen from Table 2 that the $\nabla^2\rho_{BCP}$ and H_{BCP} values at the Xe–Y BCPs in the HXeY···LiX are more positive than that in the corresponding HXeY. Thus, QTAIM analysis confirms that the ionic characteristic of the Xe–Y interaction in the dimer is reinforced with respect to the monomer. These results are consistent with the predicted trends of the Xe–Y bond distances discussed above.

3.3. Interaction energies and energy decomposition analysis

Table 3 shows the evaluated BSSE-corrected M06–2X, MP2 and CCSD(T) interaction energies of the various HXeY···LiX complexes. Estimation of the BSSE for all of the structures presented here was performed using the full counterpoise method [53]. Although all calculations predict the same trend in the relative interaction energies of the complexes under consideration, a quick look at the results reveals that MP2 interaction energies generally underestimate those of M06–2X. After comparing the results using the benchmark CCSD(T), we found that the M06–2X functional

Table 2
Calculated QTAIM parameters (in au) for HXeY and HXeY···LiX complexes.

Complex	Y···Li				H–Xe				Xe–Y			
	ρ_{BCP}	$\nabla^2\rho_{BCP}$	H_{BCP}	$-G_{BCP}/V_{BCP}$	ρ_{BCP}	$\nabla^2\rho_{BCP}$	H_{BCP}	$-G_{BCP}/V_{BCP}$	ρ_{BCP}	$\nabla^2\rho_{BCP}$	H_{BCP}	$-G_{BCP}/V_{BCP}$
HXeH	–	–	–	–	0.107	−0.066	−0.055	0.412	0.107	−0.066	−0.055	0.412
HXeH···LiH (I)	0.011	0.048	0.002	1.193	0.146	−0.187	−0.104	0.355	0.084	0.009	−0.034	0.515
HXeH···LiCN (I)	0.012	0.048	0.002	1.167	0.146	−0.196	−0.104	0.347	0.083	0.015	−0.033	0.526
HXeH···LiNC (I)	0.012	0.049	0.002	1.180	0.146	−0.197	−0.104	0.346	0.083	0.015	−0.033	0.527
HXeH···LiOH (I)	0.012	0.048	0.002	1.190	0.146	−0.190	−0.104	0.352	0.084	0.011	−0.034	0.520
HXeH···$LiNH_2$ (I)	0.011	0.048	0.002	1.193	0.146	−0.190	−0.104	0.352	0.084	0.011	−0.034	0.519
HXeH···$LiCH_3$ (I)	0.011	0.048	0.002	1.193	0.146	−0.187	−0.104	0.355	0.084	0.009	−0.034	0.515
HXeCN	–	–	–	–	0.148	−0.216	−0.107	0.331	0.074	0.072	−0.025	0.630
HXeCN···LiH (I)	0.028	0.197	0.008	1.233	0.159	−0.267	−0.122	0.312	0.062	0.084	−0.017	0.693
HXeCN···LiH (II)	0.011	0.058	0.003	1.316	0.153	−0.254	−0.113	0.306	0.066	0.089	−0.019	0.683
HXeCN···LiCN (I)	0.030	0.211	0.008	1.213	0.161	−0.277	−0.125	0.308	0.060	0.086	−0.015	0.706
HXeCN···LiCN (II)	0.013	0.069	0.003	1.286	0.155	−0.266	−0.117	0.301	0.065	0.091	−0.018	0.692
HXeCN···LiNC (I)	0.030	0.188	0.002	1.042	0.161	−0.276	−0.125	0.309	0.060	0.086	−0.015	0.705
HXeCN···LiNC (II)	0.012	0.065	0.003	1.314	0.158	−0.271	−0.120	0.305	0.065	0.091	−0.018	0.693
HXeCN···LiOH (I)	0.026	0.188	0.008	1.245	0.158	−0.262	−−0.121	0.314	0.063	0.083	−0.018	0.686
HXeCN···$LiNH_2$ (I)	0.027	0.189	0.008	1.238	0.158	−0.263	−0.121	0.314	0.063	0.084	−0.017	0.688
HXeCN···$LiCH_3$ (I)	0.027	0.188	0.007	1.199	0.159	−0.265	−0.122	0.313	0.063	0.084	−0.017	0.690
HXeNC	–	–	–	–	0.161	−0.258	−0.126	0.327	0.070	0.145	−0.020	0.737
HXeNC···LiH (I)	0.025	0.141	0.004	1.166	0.168	−0.298	−0.136	0.311	0.060	0.144	−0.013	0.790
HXeNC···LiH (II)	0.008	0.041	0.002	1.376	0.164	−0.299	−0.130	0.298	0.056	0.139	−0.010	0.811
HXeNC···LiCN (I)	0.028	0.152	0.004	1.145	0.169	−0.307	−0.137	0.306	0.058	0.144	−0.012	0.803
HXeNC···LiCN (II)	0.009	0.047	0.002	1.357	0.167	−0.296	−0.133	0.307	0.065	0.154	−0.016	0.772
HXeNC···LiNC (I)	0.027	0.152	0.004	1.149	0.169	−0.306	−0.137	0.307	0.058	0.143	−0.012	0.803
HXeNC···LiNC (II)	0.009	0.047	0.003	1.379	0.166	−0.295	−0.133	0.307	0.065	0.154	−0.016	0.771
HXeNC···LiOH (I)	0.024	0.137	0.004	1.178	0.167	−0.294	−0.135	0.312	0.061	0.145	−0.014	0.784
HXeNC···$LiNH_2$ (I)	0.025	0.138	0.004	1.170	0.168	−0.295	−0.135	0.312	0.061	0.145	−0.014	0.786
HXeNC···$LiCH_3$ (I)	0.025	0.138	0.004	1.167	0.168	−0.297	−0.135	0.311	0.060	0.145	−0.013	0.788

Table 3
Interaction energies and energy decomposition analysis (in kcal/mol) for HXeY···LiX complexes.

Complex	E_{int}^{M06-2X}	E_{int}^{MP2}	$E_{int}^{CCSD(T)}$	E_{elst}	$E_{exch-rep}$	E_{pol}	E_{disp}	% E_{elst}
HXeH								
HXeH···LiH (I)	−12.0	−11.2	−10.7	−9.9	7.1	−8.2	−1.0	52
HXeH···LiCN (I)	−16.0	−14.9	−14.1	−12.3	7.7	−10.4	−0.9	52
HXeH···LiNC (I)	−15.5	−15.0	−13.9	−12.1	7.5	−10.1	−0.8	52
HXeH···LiOH (I)	−10.4	−10.0	−9.5	−8.9	6.1	−6.7	−0.9	54
HXeH···$LiNH_2$ (I)	−10.7	−10.4	−9.8	−9.1	6.2	−6.9	−0.9	54
HXeH···$LiCH_3$ (I)	−11.3	−10.7	−10.2	−9.5	6.9	−7.6	−1.2	52
HXeCN								
HXeCN···LiH (I)	−26.0	−24.6	−24.6	−28.4	13.2	−8.2	−2.6	72
HXeCN···LiH (II)	−17.5	−15.6	−15.9	−15.2	5.34	−5.0	−2.6	66
HXeCN···LiCN (I)	−31.8	−29.8	−30.0	−33.2	13.6	−9.4	−2.8	73
HXeCN···LiCN (II)	−22.7	−19.9	−20.7	−19.7	6.0	−7.3	−2.7	67
HXeCN···LiNC (I)	−31.0	−29.9	−29.6	−32.6	13.5	−9.2	−2.7	73
HXeCN···LiNC (II)	−22.8	−20.8	−21.1	−19.2	5.9	−7.0	−2.6	67
HXeCN···LiOH (I)	−23.9	−22.5	−22.6	−25.8	11.6	−6.6	−2.5	74
HXeCN···$LiNH_2$ (I)	−23.3	−23.1	−23.1	−26.1	11.7	−6.9	−2.5	73
HXeCN···$LiCH_3$ (I)	−25.0	−23.8	−23.8	−27.3	12.7	−7.5	−2.8	73
HXeNC								
HXeNC···LiH (I)	−25.8	−26.0	−25.2	−29.3	13.9	−7.9	−2.5	74
HXeNC···LiH (II)	−16.6	−16.4	−15.9	−14.0	9.6	−4.4	−2.3	67
HXeNC···LiCN (I)	−31.7	−31.6	−30.8	−34.4	14.3	−8.9	−2.6	75
HXeNC···LiCN (II)	−22.7	−19.2	−21.4	−18.7	9.7	−6.0	−2.2	69
HXeNC···LiNC (I)	−30.9	−31.7	−30.6	−33.8	14.1	−8.7	−2.5	75
HXeNC···LiNC (II)	−22.9	−20.0	−21.6	−18.8	9.6	−6.1	−2.2	69
HXeNC···LiOH (I)	−23.3	−23.9	−23.3	−26.8	12.5	−6.5	−2.4	75
HXeNC···$LiNH_2$ (I)	−23.8	−24.5	−23.9	−27.1	12.5	−6.7	−2.5	75
HXeNC···$LiCH_3$ (I)	−24.8	−25.2	−24.5	−28.3	13.7	−7.3	−2.8	74

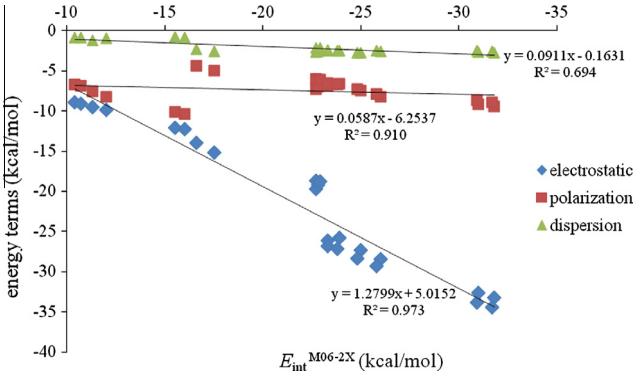

Fig. 3. Relationship between different energy terms and total interaction energies of HXeY···LiX complexes.

provided the rather reliable results for the LB interactions. From these data, it is seen that the Li···π interaction energies span over a range from −15.9 to −21.6 kcal/mol at the CCSD(T)/aug-cc-pVTZ(-PP) level of theory. Structure I was found to be the global minimum of the complexes, its interaction energy is between −9.5 and −30.8 kcal/mol at the CCSD(T)/aug-cc-pVTZ(-PP) level. For the both structures I and II, the contributions from the increased electron correlation (CCSD(T)) compared with interaction energies at the respective MP2 level are small in all cases. We could not find any theoretical information in the literature regarding the interaction energies of the HXeY···LiX complexes. However, we can compare our estimates with the interaction energies of HXeY···XCF_3, where Y = CN, NC and X = F, Cl, Br, I [61]. The MP2-estimated complexation energy for the structure I of HXeNC···LiH complex is −26 kcal/mol which is 17.5 kcal/mol more negative than that for the HXeNC···ICF_3. The interaction energy in the linear HXeCN···LiH complex is calculated to be −24.6 kcal/mol, which is larger in absolute value than that in the HCN···LiH complex (ca. −14.9 kcal/mol) [62]. The result reveals that the insertion of an Xe atom into the H–CN bond further enhances the N···Li interaction.

To further understand the nature of the LB interactions in these complexes, the interaction energies of complexes were decomposed into four parts: electrostatic interaction energy (E_{elst}), Pauli exchange-repulsion energy ($E_{exch-rep}$), polarization energy (E_{pol}) and dispersion energy (E_{disp}). The results are given in Table 3. It is seen that, for the all HXeY···LiX complexes, the dominant attractive contributions mostly originate from the electrostatic energy E_{elst}. The electrostatic forces contribute about 75% to the total attractive interaction energy for structure I of HXeCN···LiH complex and HXeNC···LiH complex. The stabilities of the lithium-π interactions are also predicted to be attributable mainly to electrostatic effects, while polarization and dispersion forces play a smaller role in stabilizing these complexes. Since the HXeY molecule has a large contribution of the $(HXe)^+Y^-$ bonding and its ionicity is enhanced in the HXeY–LiX complex, the larger electrostatic term can be explained by the dipole–dipole interaction term between the monomers. The polarization forces play a secondary role in these complexes, and contribute about 20–45% to the total attractive interaction energy. Compared with electrostatic and polarization energies, the dispersion energy (E_{disp}) is rather small. For the same type of the complex, the $E_{exch-rep}$ becomes more positive in the order $NH_2 < CH_3 < OH < H < NC < CN$, maybe this is due to the increased overlap between the orbitals of the two monomers. To elucidate the role of each energy term, we have plotted the magnitude of the individual interaction energy component of structure I versus the total interaction energy (Fig. 3). This reveals that the electrostatic interactions are essentially responsible for the substituent effects on the magnitude of the LB in HNgY···LiX complexes. This finding is in line with the previous interaction energy decomposition analysis of HNgY complexes [41].

4. Conclusion

Theoretical calculations were performed for the HXeY···LiX (X = H, CN, NC, OH, NH_2, CH_3; Y = H, CN and NC) complexes and

the respective HXeY monomers with the MP2, M06–2X and CCSD(T) methods. The following conclusions are found. The global minimum for the HXeY···LiX complex was found on the potential energy surface for the configuration I, i.e. the structure of a linear Xe–Y···Li interaction. The predicted LB distances of structures I are in a range of 1.854–1.922, 1.977–2.019 Å and 2.109–2.150 Å for HXeH···LiX, HXeCN···LiX and HXeNC···LiX complexes, respectively. These are much smaller than the sum of Van der Waals radii for counterpart atoms, which reveals the existence of the relatively strong interaction between HXeY and LiX molecules. The evaluated Li···π bond distances of configuration II are in the range of 2.339–2.535 Å (MP2) and 2.291–2.490 Å (M06). One can see that, the H–Xe stretching mode of HXeY molecules shifts upon complexation higher in energy, i.e. exhibits a blue shift. The blue shifts of the Xe–H stretching mode are attributed to the enhancement of the $(HXe)^{+}Y^{-}$ ion-pair character upon complexation. Also the large increase of the H−Xe intensity of the HXeH···LiX compared with the isolated HXeH must be noted. The redistribution of the electron density at H–Xe critical points upon complex formation is also noticeable. The electron densities at the H–Xe BCPs in the HXeY···LiX complexes are slightly larger than those of HXeY molecules. This result is in agreement with the observed blue shift of the stretching and the shortening of the H–Xe bond upon complexation. Moreover, QTAIM analysis confirms that the ionic characteristic of the Xe–Y interaction in the dimer is reinforced with respect to the monomer. From the energy decomposition analysis results, it is concluded that for the all HXeY···LiX complexes, the dominant attractive contributions mostly originate from the electrostatic energy.

Appendix A. Supplementary material

Supplementary material associated with this article can be found, in the online version, at http://dx.doi.org/10.1016/j.comptc.2013.10.026.

References

[1] G.R. Desiraju, T. Steiner, The Weak Hydrogen Bond, Oxford University Press, Oxford, 1999.
[2] K.E. Riley, P. Hobza, Noncovalent interactions in biochemistry, Wiley Interdiscip. Rev. Comput. Mol. Sci. 1 (2011) 3–17.
[3] S. Scheiner, Hydrogen Bonding: A Theoretical Prospective, Oxford University Press, Oxford, UK, 1997.
[4] M.D. Esrafili, H. Behzadi, J. Beheshtian, N.L. Hadipour, Theoretical 14N nuclear quadrupole resonance parameters for sulfa drugs: Sulfamerazine and sulfathiazole, J. Mol. Graph. Model. 27 (2008) 326–331.
[5] P. Politzer, J.S. Murray, M.C. Concha, Halogen bonding and the design of new materials: organic bromides, chlorides and perhaps even fluorides as donors, J. Mol. Model. 13 (2007) 643–650.
[6] M.D. Esrafili, A theoretical investigation of the characteristics of hydrogen/halogen bonding interactions in dibromo-nitroaniline, J. Mol. Model. 19 (2013) 1417–1427.
[7] R.H. Crabtree, P.E.M. Siegbahn, O. Eisenstein, A.L. Rheingold, A new intermolecular interaction: unconventional hydrogen bonds with element−hydride bonds as proton acceptor, Acc. Chem. Res. 29 (1996) 348–354.
[8] I. Alkorta, K. Zborowski, J. Elguero, M. Solimannejad, Theoretical study of dihydrogen bonds between $(XH)_2$, X = Li, Na, BeH, and MgH, and weak hydrogen bond donors (HCN, HNC, and HCCH), J. Phys. Chem. A 110 (2006) 10279–10286.
[9] I. Alkorta, J. Elguero, M. Solimannejad, S.J. Grabowski, Dihydrogen bonding vs metal-σ interaction in complexes between H_2 and metal hydride, J. Phys. Chem. A 115 (2011) 201–210.
[10] T.T. Bui, S. Dahaoui, C. Lecomte, G.R. Desiraju, E. Espinosa, The nature of halogen halogen interactions: a model derived from experimental charge-density analysis, Angew. Chem. Int. Ed. 48 (2009) 3838–3841.
[11] G. Cavallo, P. Metrangolo, T. Pilati, G. Resnati, M. Sansotera, G. Terraneo, Halogen bonding: a general route in anion recognition and coordination, Chem. Soc. Rev. 39 (2010) 3772–3783.
[12] B.S. Ault, G.C. Pimentel, Matrix isolation infrared studies of lithium bonding, J. Phys. Chem. 79 (1975) 621–626.
[13] S. Scheiner, E.A.M. Sapse, P.R. Schleyer, Recent Studies in Lithium Chemistry: A Theoretical and Experimental Overview, John Wiley & Sons Inc, New York, 1995.
[14] S.S.C. Ammal, P. Venuvanalingam, Π-Systems as lithium/hydrogen bond acceptors: some theoretical observations, J. Chem. Phys. 109 (1998) 9820–9830.
[15] Q.Z. Li, Y.F. Wang, W.Z. Li, J.B. Cheng, B.A. Gong, J.Z. Sun, Prediction and characterization of the HMgH LiX (X = H, OH, F, CCH, CN, and NC) complexes: a lithium–hydride lithium bond, Phys. Chem. Chem. Phys. 11 (2009) 2402–2407.
[16] M. Solimannejad, S. Ghafari, M.D. Esrafili, Theoretical insight into cooperativity in lithium-bonded complexes: linear clusters of LiCN and LiNC, Chem. Phys. Lett. 577 (2013) 6–10.
[17] L. Khriachtchev, M. Pettersson, N. Runeberg, J. Lundell, M. Räsänen, A stable argon compound, Nature 406 (2000) 874–876.
[18] M. Pettersson, J. Lundell, L. Khriachtchev, M. Räsänen, Neutral rare-gas containing charge-transfer molecules in solid matrices III. HXeCN, HXeNC, and HKrCN in Kr and Xe, J. Chem. Phys. 109 (1998) 618–625.
[19] L. Khriachtchev, M. Räsänen, R.B. Gerber, Noble-gas hydrides: new chemistry at low temperatures, Acc. Chem. Res. 42 (2009) 183–191.
[20] M. Pettersson, J. Lundel, M. Räsänen, New rare-gas-containing neutral molecules, Eur. J. Inorg. Chem. 1999 (1999) 729–737.
[21] M. Pettersson, J. Lundell, M. Räsänen, Neutral rare-gas containing charge-transfer molecules in solid matrices I. HXeCl, HXeBr, HXeI, and HKrCl in Kr and Xe, J. Chem. Phys. 102 (1995) 642–6431.
[22] M. Pettersson, J. Lundell, M. Räsänen, Neutral rare-gas containing charge-transfer molecules in solid matrices II. HXeH, HXeD, and DXeD in Xe, J. Chem. Phys. 103 (1995) 205–210.
[23] M. Pettersson, L. Khriachtchev, A. Lignell, M. Räsänen, HKrF in solid krypton, J. Chem. Phys. 116 (2002) 2508–2515.
[24] G. Frenking, Chemistry: another noble gas conquered, Nature (London) 406 (2000) 836–837.
[25] R.B. Gerber, Formation of novel rare-gas molecules in low-temperature matrixes, Annu. Rev. Phys. Chem. 55 (2004) 55–78.
[26] V.I. Feldman, F.F. Sukhov, Formation and decay of transient xenon dihydride resulting from hydrocarbon radiolysis in a xenon matrix, Chem. Phys. Lett. 255 (1996) 425–430.
[27] A. Lignell, L. Khriachtchev, M. Pettersson, M. Räsänen, Interaction of rare-gas-containing molecules with nitrogen: Matrix-isolation and ab initio study of HArF···N_2, HKrF···N_2, and HKrCl···N_2 complexes, J. Chem. Phys. 118 (2003) 11120–11128.
[28] H. Tanskanen, S. Johansson, A. Lignell, L. Khriachtchev, M. Räsänen, Matrix isolation and ab initio study of the HXeCCH···CO_2 complex, J. Chem. Phys. 127 (2007) 154313.
[29] L. Khriachtchev, S. Tapio, M. Räsänen, A. Domanskaya, A. Lignell, HY···N_2 and HXeY···N_2 complexes in solid xenon (Y = Cl and Br): unexpected suppression of the complex formation for deposition at higher temperature, J. Chem. Phys. 133 (2010) 084309.
[30] M. Tsuge, S. Berski, M. Räsänen, Z. Latajka, L. Khriachtchev, Experimental and computational study of the HXeI HY complexes (Y = Br and I), J. Chem. Phys. 138 (2013) 104314.
[31] A. Lignell, J. Lundell, L. Khriachtchev, M. Räsänen, Experimental and computational study of HXeY HX somplexes (X, Y = Cl and Br): an example of exceptionally large complexation effect, J. Phys. Chem. A 112 (2008) 5486–5494.
[32] J. Cheng, Y. Wang, Q. Li, Z. Liu, W. Li, B. Gong, Gigantic blue shift of the H–Ar stretch vibration in π hydrogen-bonded C2H2 HArCCF complex, J. Phys. Chem. A 113 (2009) 5235–5239.
[33] M.D. Esrafili, M. Solimannejad, Revealing substitution effects on the strength and nature of halogen–hydride interactions: a theoretical study, J. Mol. Model. 19 (2013) 3767–3777.
[34] S.A.C. McDowell, Blue-shifting hydrogen bonding in N_2···HKrF, J. Chem. Phys. 118 (2003) 7283–7287.
[35] S.A.C. McDowell, A computational study of hydrogen-bonded complexes of HKrCl: N_2···HKrCl, OC···HKrCl, and HF···HKrCl, J. Chem. Phys. 119 (2003) 3711–3716.
[36] S.A.C. McDowell, A computational study of the hydrogen-bonded complexes FArH···OCO and FKrH···OCO, Chem. Phys. Lett. 406 (2005) 228–231.
[37] S.A.C. McDowell, A computational study of the dihydrogen bonded complexes HBeH···HArF and HBeH···HKrF, J. Chem. Phys. 121 (2004) 5728–5732.
[38] S.A.C. McDowell, Comparison of the intermolecular properties of N_2···HArF with N_2···HF, J. Chem. Phys. 118 (2003) 4066–4072.
[39] S.A.C. McDowell, Harmonic vibrational blue shifts in FXeH···Y complexes (Y = N2 CO., BF and HF) predicted by a perturbative model, Chem. Phys. 328 (2006) 69–74.
[40] S.A.C. McDowell, Studies of neutral rare-gas compounds and their non-covalent interactions with other molecules, Curr. Org. Chem. 10 (2006) 791–803.
[41] A. Lignell, L. Khriachtchev, Intermolecular interactions involving noble-gas hydrides: where the blue shift of vibrational frequency is a normal effect, J. Mol. Struct. 889 (2008) 1–11.
[42] S.A.C. McDowell, Blue shifting and red shifting hydrogen bonds: a study of the $HArFN_2$ and $HArFP_2$ complexes, Phys. Chem. Chem. Phys. 5 (2003) 808–811.
[43] S.A.C. McDowell, Redshift and blueshift of the Ar–H vibrational stretching frequency in complexes of FArH and acetylene, J. Chem. Phys. 122 (2005) 204309.

[44] A. Corani, A. Domanskaya, L. Khriachtchev, M. Räsänen, A. Lignell, Matrix-isolation and ab initio study of the HKrCl HCl complex, J. Phys. Chem. A 113 (2009) 10687–10692.
[45] I.V. Alabugin, M. Manoharan, F.A. Weinhold, Blue-shifted and red-shifted hydrogen bonds in hypervalent rare-gas FRg−H Y sandwiches, J. Phys. Chem. A 108 (2004) 4720–4730.
[46] A. Lignell, L. Khriachtchev, M. Pettersson, M. Räsänen, Large blueshift of the H–Kr stretching frequency of HKrCl upon complexation with N_2, J. Chem. Phys. 117 (2002) 961–964.
[47] M. Tsuge, S. Berski, R. Stachowski, M. Räsänen, Z. Latajka, L. Khri- achtchev, High kinetic stability of HXeBr upon interaction with carbon dioxide: HXeBr···CO_2 complex in a Xenon matrix and HXeBr in a carbon dioxide matrix, J. Phys. Chem. A 116 (2012) 4510-4517.
[48] A. Domanskaya, A.V. Kobzarenko, E. Tsivion, L. Khriachtchev, V.I. Feldman, R.B. Gerber, M. Räsänen, Matrix-isolation and ab initio study of HXeCCH complexed with acetylene, Chem. Phys. Lett. 481 (2009) 83–87.
[49] A.V. Nemukhin, B.L. Grigorenko, L. Khriachtchev, H. Tanskanen, M. Pettersson, M. Räsänen, Intermolecular complexes of HXeOH with water: stabilization and destabilization effects, J. Am. Chem. Soc. 124 (2002) 10706–10711.
[50] A. Lignell, L. Khriachtchev, M. Pettersson, M. Räsänen, Interaction of rare-gas-containing molecules with nitrogen: Matrix-isolation ab initio study of HArF···N_2 HKrF···N_2 and HKrCl···N_2 complexes, J. Chem. Phys. 118 (2003) 11120–11128.
[51] M.W. Schmidt, K.K. Baldridge, J.A. Boatz, S.T. Elbert, M.S. Gordon, J.H. Jensen, S. Koseki, N. Matsunaga, K.A. Nguyen, S.J. Su, T.L. Windus, M. Dupuis, J.A. Montgomery, General atomic and molecular electronic structure system, J. Comput. Chem. 14 (1993) 1347–1363.
[52] K.A. Peterson, D. Figgen, E. Goll, H. Stoll, M. Dolg, Systematically convergent basis sets with relativistic pseudopotentials. II. Small-core pseudopotentials and correlation consistent basis sets for the post-d group 16–18 elements, J. Chem. Phys. 119 (2003) 11113–11123.
[53] S.F. Boys, F. Bernardi, The calculation of small molecular interactions by the differences of separate total energies. Some procedures with reduced errors, Mol. Phys. 19 (1970) 553–566.
[54] R.F.W. Bader, Atoms in Molecules-A Quantum Theory, Oxford University Press, New York, 1990.
[55] F. Biegler-Konig, J. Schonbohm, D. Bayles, AIM2000-a program to analyze and visualize atoms in molecules, J. Comput. Chem. 22 (2001) 545–559.
[56] P. Su, H. Li, Energy decomposition analysis of covalent bonds and intermolecular interactions, J. Chem. Phys. 131 (2009) 014102.
[57] A. Bondi, Van der Waals volumes and radii, J. Phys. Chem. 68 (1964) 441–451.
[58] I. Rozas, I. Alkorta, I. Elguero, Behaviour of ylides containing N, O and C atoms as hydrogen bond acceptors, J. Am. Chem. Soc. 122 (2000) 11154–11161.
[59] M.D. Esrafili, Characteristics and nature of the intermolecular interactions in boron-bonded complexes with carbene as electron donor: an ab initio, SAPT and QTAIM study, J. Mol. Model. 18 (2012) 2003–2011.
[60] M.D. Esrafili, B. Ahmadi, A theoretical investigation on the nature of Cl···N and Br···N halogen bonds in F-Ar–X···NCY complexes (X = Cl, Br and Y = H, F, Cl, Br, OH, NH2, CH3 and CN), Comput. Theor. Chem. 997 (2012) 77–82.
[61] M.D. Esrafili, S. Shahabivand, E. Vessally, HRgCN and HRgNC as halogen bond acceptors (Rg = Kr and Xe): A theoretical study upon strength and nature of halogen···nitrogen and halogen···carbon interactions, Comput. Theor. Chem. 1020 (2013) 1–6.
[62] Q. Li, T. Hu, X. An, W. Li, J. Cheng, B. Gong, J. Sun, Theoretical study of the interplay between lithium bond and hydrogen bond in complexes involved with HLi and HCN, Chem. Phys. Chem. 10 (2009) 3310–3315.